Report

Current Biology

Evolution of a remarkable intracellular polymer and extreme cell allometry in hagfishes

Graphical abstract

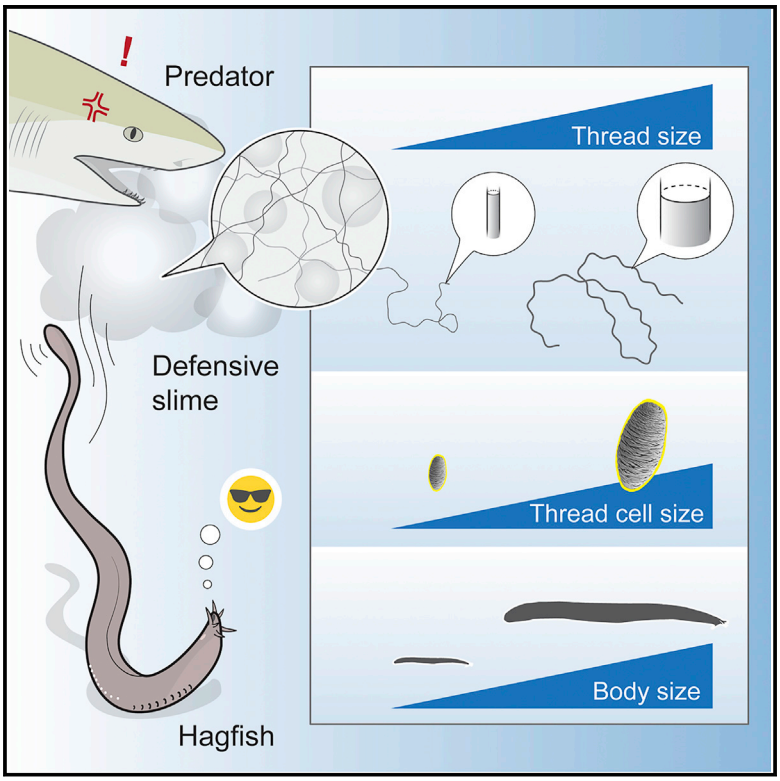

Authors

Yu Zeng, Skylar Petrichko, Kristen Nieders, David Plachetzki, Douglas Fudge

Correspondence

yzeng@chapman.edu

In brief

Animal cell size rarely changes with body size. Zeng et al. show that hagfish gland thread cells vary by 50-fold in volume as body length varies between 10 and 128 cm. Larger hagfishes have disproportionally larger gland thread cells to produce and store longer and thicker slime threads, which likely help defend against more powerful predators.

Highlights

- Hagfish gland thread cells vary between 40 and 250 μm in length and 50-fold in volume
- Larger gland thread cells are found in larger hagfishes and produce larger threads
- Longer and thicker threads likely help defend against larger predators
- Hagfish slime threads are by far the largest intracellular polymers known

Zeng et al., 2021, Current Biology *31*, 5062–5068
November 22, 2021
https://doi.org/10.1016/j.cub.2021.08.066

CellPress

CellPress

Current Biology

Report

Evolution of a remarkable intracellular polymer and extreme cell allometry in hagfishes

Yu Zeng,[1,3,6,*] Skylar Petrichko,[1] Kristen Nieders,[1] David Plachetzki,[2,4] and Douglas Fudge[1,5]
[1]Schmid College of Science and Technology, Chapman University, 1 University Drive, Orange, CA 92866, USA
[2]Department of Molecular, Cellular, & Biomedical Sciences, University of New Hampshire, 105 Main Street, Durham, NH 03824, USA
[3]Twitter: @yuzenghiking
[4]Twitter: @plachetzki
[5]Twitter: @douglasfudge
[6]Lead contact
*Correspondence: yzeng@chapman.edu
https://doi.org/10.1016/j.cub.2021.08.066

SUMMARY

The size of animal cells rarely scales with body size, likely due to biophysical and physiological constraints.[1,2] In hagfishes, gland thread cells (GTCs) each produce a silk-like proteinaceous fiber called a slime thread.[3,4] The slime threads impart strength to a hagfish's defensive slime and thus are potentially subject to selection on their function outside of the body.[5–8] Body size is of fundamental importance in predator-prey interactions, which led us to hypothesize that larger hagfishes produce longer and stronger slime threads than smaller ones.[9] Here, by sampling a range of sizes of hagfish from 19 species, we systematically examined the scaling of GTC and slime-thread dimensions with body size within both phylogenetic and ontogenetic contexts. We found that the length of GTCs varied between 40 and 250 μm and scaled positively with body size, exhibiting an allometric exponent greater than those in other animal cells. Correspondingly, larger hagfishes produce longer and thicker slime threads and thus are equipped to defend against larger predators. With diameter and length varying 4-fold (0.7–4 μm and 5–22 cm, respectively) over a body-size range of 10–128 cm, the slime threads characterize the largest intracellular polymers known in biology. Our results suggest selection for stronger defensive slime in larger hagfishes has driven the evolution of extreme size and allometry of GTCs.

RESULTS

Hagfishes are deep-sea animals whose primary defense from predators relies on the ejection of subcellular products from epidermal glands.[5] When attacked, hagfishes produce a defensive slime that expands rapidly to clog the predator's mouth and gills.[6–8] The impressive strength of the slime is imparted by a complex network of slime threads that entrains seawater with mucus. The slime threads are proteinaceous fibers, individually produced and stored within highly specialized gland thread cells (GTCs) as a densely packed skein (Figure 1A).[3,4] Slime threads consist mainly of fibrous α and γ proteins from the intermediate filament (IF) family, and they rival spider silk in their strength and toughness.[10–14]

Hagfish body size varies substantially within and among species. As direct developers, newly hatched hagfish juveniles could be as small as 4 cm in length.[16] By sampling from the two most speciose genera, *Eptatretus* and *Myxine*, we show that the maximum length (L_{max}) of adults varies between species, ranging from ~20 to ~128 cm. Also, L_{max} is not phylogenetically conserved, with various sized species found in both genera and from different oceans (Figures 1B–1D). Ancestral state reconstruction suggests an intermediate ancestral body size of L_{max} ~50 cm, followed by repeated evolutionary increases and reductions (Figure S1B). By addressing the variations of GTC size and thread dimension with respect to body size, we aim to reveal the general scaling patterns in hagfish ontogeny and evolution and test the main hypothesis that larger hagfishes possess larger slime threads to defend against larger predators.

Extreme size and allometry of GTCs

We examined the scaling of GTC size with body size for the presence of significant allometry. To analyze how the volume of GTCs (as represented by the thread skein) scales with body size, we first sampled their dimensions from 19 hagfish species with different body sizes. We found that body length (L; ranging 9.4–71.5 cm) scaled with body mass (M) with a mean allometric exponent of ~0.44 (Figure S1C):

$$L \propto M^{0.44}. \quad \text{(Equation 1)}$$

The length of GTC skeins (L_S; i.e., the major axis) varied from 50.1 to 277.6 μm, and the GTC skein width (W_S) varied from 40.0 to 184.4 μm (Figure S3A). Weak phylogenetic signals were found in L and L_S, reflecting large differences in body size among closely related species (Table S1).

We found larger thread skeins in larger hagfishes. Across all sampled species, L_S of the largest skeins (top 20% of each individual hagfish), and L were positively correlated (Generalized least-squares regression, $p < 0.0001$), with the mean power-law exponent ~0.37 (Figure 2A; Table S3):

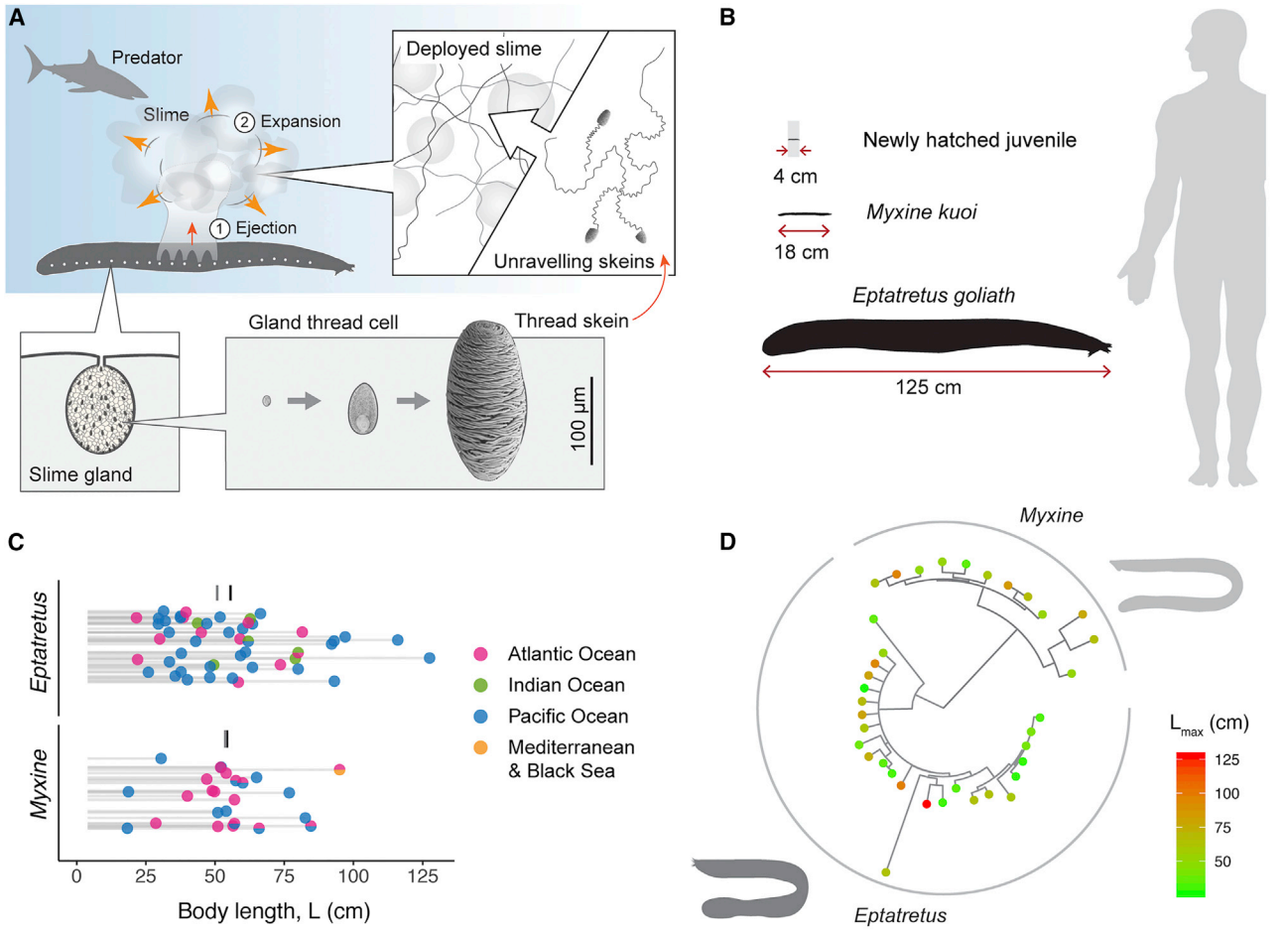

Figure 1. Defensive function of hagfish slime threads and body-size variation in hagfishes

(A) Hagfish slime originates within epidermal slime glands (bottom left) and is reinforced by silk-like threads that are produced within gland thread cells, which undergo a massive change in size during maturation (bottom right). Predator attacks (top left) induce ejection of exudate from slime glands, followed by hydration of mucus and unraveling of coiled slime threads in seawater, which results in a rapid increase in volume by ~10,000 times within <1 s (top right).

(B) A demonstration of inter- and intra-specific variations of body length using the contrast between newly hatched juvenile, an adult of a small species and an adult of a large species.

(C) Summary of interspecific body-size variation in the two most speciose genera, *Eptatretus* and *Myxine*, which together comprise 79 of 87 known species. Dots represent maximum body length (L_{max}), and gray lines represent the range of variation from juvenile (~4 cm) to adult. Colors represent geographic distribution. Vertical lines represent genus-specific means (black) and medians (gray).

(D) Mapping of L_{max} for all sampled species on a recent phylogeny[15] shows that body size is not phylogenetically conserved (see also Figure S1B and Data S1).

$$L_S \propto L^{0.37}. \quad \text{(Equation 2)}$$

This scaling relationship is further supported by the results of the MCMCglmm analyses, where a significant correlation between L_S and L was found after accounting for phylogeny and intraspecific body-size variation (Table S2). With the scaling of body length with mass (Figure S3C), we further derived the allometry of L_S as $L_S \propto M^{0.16}$. At the ontogenetic scale, L_S also increases with increasing body size, as demonstrated in Atlantic hagfish (*M. limosa*) (L_S varied from 80 to 160 μm over the L size range of ~20 to 60 cm; Figure 2A, inset; Figure S2B).

The ellipsoidal shape of GTC skeins was relatively consistent within each species. Among all species, the mean aspect ratio of skeins (*AR*; i.e., the ratio of skein length L_S to width W_S) varied between 1.6 and 2.5 and showed significant interspecific variation (ANOVA, $F_{18,2267} = 33.64$, $p < 0.0001$ for top 20% skeins; Figure S3A). Animal-specific *AR* was later incorporated into the estimation of thread length (see below).

The estimated volume (V_S) of GTCs ranged $1 \times 10^{4.6}$–$1 \times 10^{6.3}$ μm^3, with the largest ones being ~50 times larger than the smallest ones. Notably, the largest GTCs are some of the largest vertebrate cells, about 1–5 orders of magnitude larger than most other cells (Figure S3G). The production and storage of large threads may have played a key role in the large size of GTCs (see Discussion). Among all hagfishes, V_S scaled with body size *L* with an exponent of 1.32 ($V_S \propto L^{1.32}$; Figure S3B) and exhibited a large scaling exponent ~0.55 with body mass:

$$V_S \propto M^{0.55}. \quad \text{(Equation 3)}$$

This indicates an extreme allometry compared to the several kinds of mammalian cells in which scaling with body size has

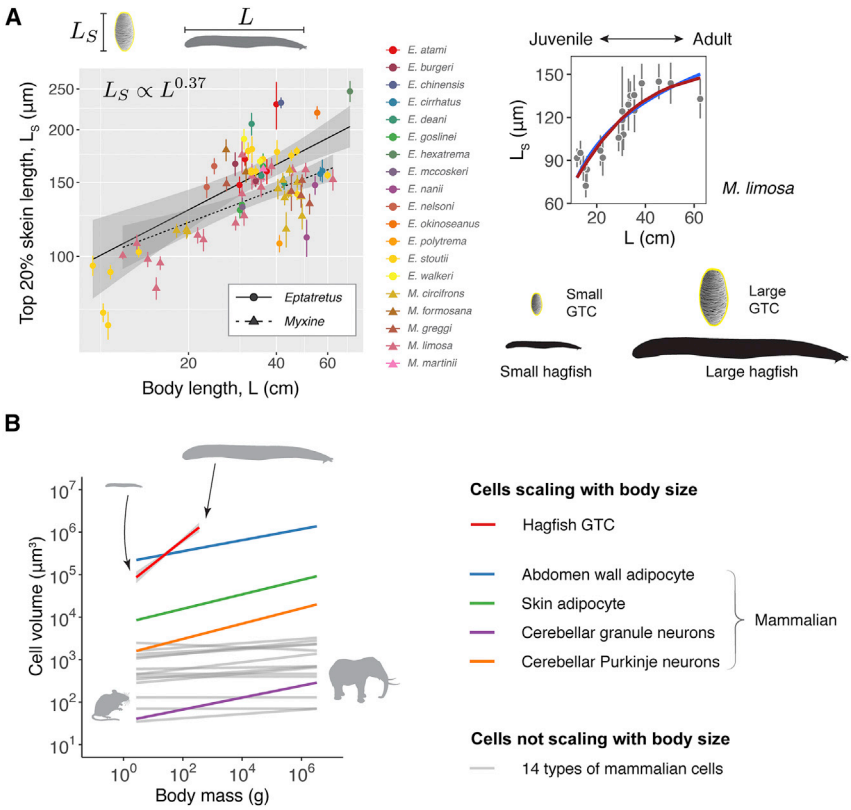

Figure 2. Hagfish gland thread cells exhibit extreme allometry

(A) GTC size, as represented by thread skein length (L_S), is positively correlated with body length (L). Plot shows L_S from the largest 20% of GTCs sampled from each hagfish versus L (means ± SD), with a scaling exponent 0.37 ± 0.04 for both genera combined (0.42 ± 0.06 for *Eptatretus* and 0.30 ± 0.05 for *Myxine*). Marker shapes represent different genera; colors represent different species; trend lines represent logarithmic regression models for two genera, with shaded gray representing SEM. Inset to the right shows the ontogenetic variation of L_S with respect to L in one species (*M. limosa*), with trend lines representing logarithmic regression model (blue) and Gompertz growth curve (red) (see also Figures S2B and S2C).

(B) A comparison of cell allometry between hagfish GTCs and mammalian cells, sampled across a size range from mice to elephant. Most mammalian cells show little to no allometry (exponent <0.08, gray lines), and only four types of cells exhibit significant allometry (exponent 0.13–0.18). GTCs are not only much larger than most other cells but also exhibit an extreme allometry, with exponent ~0.55 (red line, with the shade representing SEM). A preliminary sampling of other hagfish cells also revealed allometry in other cells, while the GTCs exhibited the largest scaling exponent (Figure S3; Data S1).

been examined (Figure 2B).[17] Also, the scaling exponent for GTCs is much higher than those of skin adipocytes and hepatocytes (Figures S3D and S3E). Strong scaling of GTC size with body size supports our hypothesis that selection for greater *ex vivo* defensive function can influence the size of the cells responsible for that function over evolutionary timescales.

Scaling of thread diameter and length

Integrating thread diameter measurements and geometric models, we further derive the scaling relationship between slime thread and body size. We found that slime-thread dimensions increase with increasing skein size and body size. The maximum thread diameter (ϕ_{max}; sampled at the midpoint of skeins; Figure S1E) positively correlates with skein length (L_S), with the mean power-law exponent ~1.04 (Figure 3A), as described by

$$\phi_{max} \propto L_S^{1.04}. \quad \text{(Equation 4)}$$

This indicates a near-isometric scaling of thread diameter with skein size ($\phi_{max} \propto L_S$) and rejects the alternative hypothesis of consistent thread length (i.e., $\phi_{max} \propto L_S^{1.5}$; STAR Methods). This correlation was phylogenetically robust and not influenced by the intraspecific variation of skein size (Table S3). Next, we derived the general scaling of thread length (L_T) with skein length (L_S):

$$L_T \propto \frac{L_S^3}{\phi_{max}^2} = L_S^{0.92}. \quad \text{(Equation 5)}$$

Approximating the covariation of thread diameter and length with respect to skein length L_S (Equation 22), we found that the thread dimensions vary approximately linearly with skein size. For example, when L_S increases by ~2 times, both ϕ_{max} and L_T increase by ~2 times (Figure 3B).

Last, combining the scaling models above, we uncovered how thread dimensions vary with body size. Combining the general scaling models of thread diameter, skein length, and body length (Equations 9 and 12), we derived the scaling of thread diameter ϕ_{max} with body length:

$$\phi_{max} \propto L^{0.38}. \quad \text{(Equation 6)}$$

Similarly, we found the scaling of L_T with body length and mass:

$$L_T \propto L^{0.34}$$

$$\propto M^{0.15}. \quad \text{(Equation 7)}$$

These models predict that slime-thread length varies from ~11 to ~20 cm over the body-size range of ~20 to ~128 cm, with thread cross-sectional area increasing 4-fold (Figure 3C). Within a functional context, the relative thread length (Q = L_T/L) decreases with increasing body size ($Q \propto L^{-0.66}$; Figure 3D). As body size increases from 20 to 128 cm, relative thread length is reduced from ~0.55 to ~0.16 L.

DISCUSSION

Our results suggest that selection on the dimensions and mechanical performance of slime threads has favored larger slime

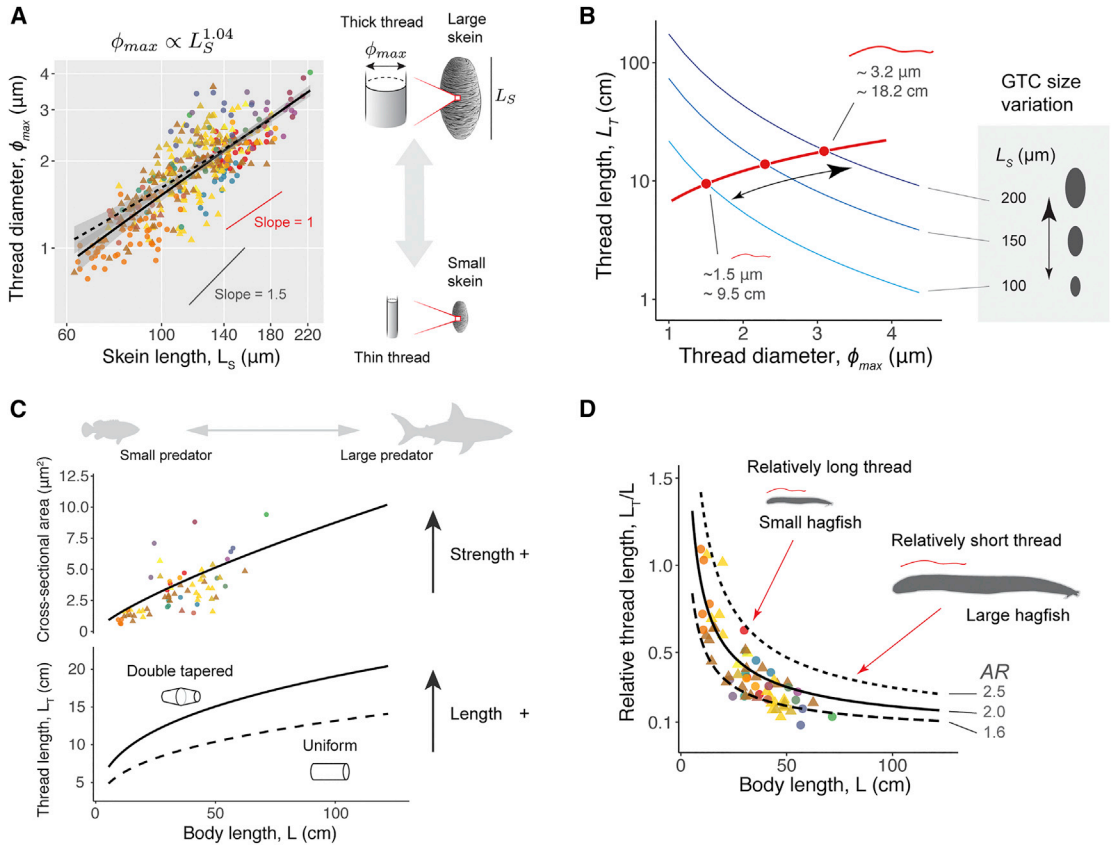

Figure 3. Slime-thread dimensions scale with body size

(A) Maximum thread diameter (ϕ_{max}; sampled from midpoint of each skein) and skein length (L_S) were positively correlated, with a mean slope of 1.04 ± 0.03 (*Myxine*, 0.97 ± 0.06; *Eptatretus*, 1.09 ± 0.04; mean ± SEM; $p < 0.0001$ for all correlations; Table S3). Points represent ϕ_{max} of individual skeins (5–10 per animal); colors represent different species (Figure 2A). Slope 1.5 represents the alternative model assuming constant thread diameter ϕ = 2 μm.

(B) A generalized model for the scaling of thread size and geometry with skein size. The red line represents the covariation of thread length (L_T) and thread diameter (ϕ_{max}) over the full range of skein sizes measured. Isolines (in blue) demonstrate the tradeoff between L_T and ϕ_{max} when thread volume is held constant for three different skein sizes. Double-tapered thread shape, ellipsoidal skein shape, and *AR* = 2 were assumed here.

(C) By combining two power-law scaling models ($\phi \sim L_S$, A; $L_S \sim L$; B), we generalized the scaling of cross-sectional area (top) and thread length (L_T; bottom) with body size (L), suggesting larger hagfishes are equipped with stronger threads against more powerful predators. For the bottom panel, line types represent two different thread geometry models (shown with longitudinally condensed cartoons of threads; see also Figure S4B). *AR* = 2 was assumed here.

(D) The relative thread length Q (i.e., the ratio of L_T to L) decreases with increasing body size. Larger hagfishes thus produce shorter threads relative to their body size (Figures 4B and 4C). Line styles represent three different skein aspect ratios (*AR*) across the full range of variation (see Figure S3A). Colored dots are mean estimated Q based on the top 20% largest skeins from individual hagfishes, with animal-specific skein *AR* incorporated. Colors represent different species; point shapes represent genus (Figure 2A; Data S1).

threads in larger hagfishes, which in turn has fostered the evolution of extreme size and allometry of GTCs (Figure 4A). Although how hagfishes interact with predators, especially different sized predators, remains under-documented, our results are consistent with the general pattern that larger prey tend to interact with larger predators.[9] Our phylogenetic analyses show a high rate of body-size evolution and repeated increases and reductions of the maximum body size on the phylogeny. Such variation in body size is likely driven by niche partitioning according to depth (e.g., ranging from <10 to 2,743 m),[18] substrate type, and resource availability. In addition, ontogenetic and sexual variation of habitat choice[19] may further increase interactions with different predators at the intraspecific level.

Evolution of extreme cell allometry

We propose that selection for larger threads in larger hagfishes has driven the extreme allometry of GTCs (Figure 2B). This can be visualized as the increase of cell size in lineages that are gaining body size (Figure 4B), which require overcoming some of the physiological, developmental, and biophysical constraints on cell size.[1] Conversely, the relaxation of such selection in lineages with decreasing body size would lead to smaller GTCs and threads.

The extreme scaling of GTCs and slime threads are perhaps less surprising considering the mechanical function of the slime threads and the numerous examples in other biomechanical systems. The allometric exponent of thread length, ~0.34 to body size or ~0.15 to body mass (Figure 3) is comparable to those

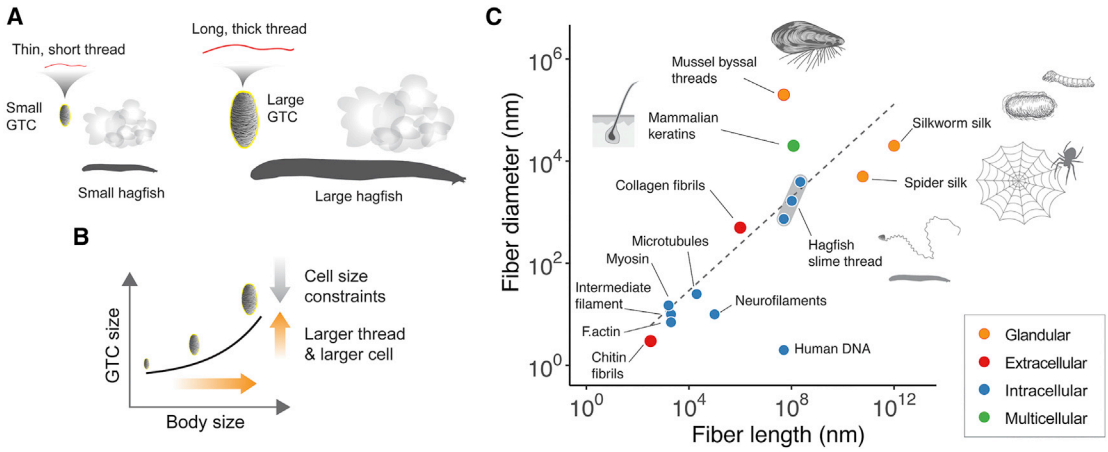

Figure 4. Selection for stronger slime underlies the extreme sizes and allometries of gland thread cells and slime threads

(A) Schematic summary for the evolutionary and ontogenetic correlations of hagfish GTCs and slime threads with body size.

(B) Schematic demonstration for the evolution of large size and extreme allometry as driven by body-size-dependent selection. The selection for larger slime threads in larger hagfishes (orange arrows) drives the size of GTCs to increase, opposing constraints on cell size.

(C) Hagfish slime threads are by far the largest intracellular polymers known, rivaling the dimensions of other biofibers produced via glandular or multicellular mechanisms. The plot shows maximum diameters and lengths for a variety of biofibers (Data S1E), with colors denoting the production mechanisms (orange, glandular; red, extracellular; blue, intracellular; green, from an assembly of multiple cells). Three dots for hagfish slime thread cover the full range of variations revealed in this study (length ~5 to ~22 cm; maximum diameter ~0.7 μm to ~3.9 μm). Trend line represents a linear regression model based on all data points excluding human DNA. See also Data S1.

seen in other systems. For example, in animals that use adhesive pads for climbing, these structures exhibit a scaling exponent of ~0.35 for pad dimension to body mass.[20] In mammals, the thickness of articular cartilage scales with body size with an exponent of 0.337, which results in a conservation of stress within structures from mice to elephants.[21] In spiders, the diameter of dragline silks scales with body mass with an exponent ranging between 0.37 and 0.39, which provides greater breaking force in larger spiders.[22]

At the cellular scale, the allometric exponent ~0.55 in GTCs far exceeds any known cases (Figure 2B). Previously, significant scaling has also been reported from defensive cells. In anemones, nematocyst cells exhibit a positive, albeit relatively weak allometry, with scaling exponents ranging from 0.008 to 0.051 with respect to body mass.[23] Our data also show that hagfish cells possess different allometries from mammalian cells, including two cell types with scaling exponent 0.24–0.26 with respect to body mass (Figures S3D and S3E). This indicates potentially taxon-specific patterns of cell allometry, which should be explored further in future work.

Functional significance

We found that slime-thread dimensions generally scaled isometrically, rather than showing a trade-off between length and diameter, with thread diameter and length both increasing by a factor of four over a skein size range of 60–220 μm (Figures 3A and 3B). Larger threads would reinforce the defensive ability of slime in several potential ways. First, with diameters four times larger, the largest threads should be able to withstand 16 times more force than the smallest threads before they fail. Assuming the thread density is conserved in slime (~27,000 per liter),[5] slime from larger hagfishes would therefore be stronger and stiffer than slime from smaller ones, and thus better at gill-clogging and resisting the hydrodynamic dislodging forces generated by larger predators. Second, longer threads likely result in larger volumes of slime, which presumably are needed to effectively deter larger predators. Third, longer threads should be able to span across wider gaps between adjacent gill arches or rakers[6,8] and thus should be more effective against larger predators. Further data on the scaling of slime production and slime gland dimensions with hagfish body size will be required to address the functional correlates of size variation in slime threads, including the reduction in relative thread length in larger hagfishes (Figure 3D).

Development of slime thread and GTCs

The selection for reinforced defensive ability has made hagfish slime threads by far the largest intracellular fiber. In most animal cells, IF proteins assemble into flexible 10-nm filaments that are involved in mechanical reinforcement (e.g., mammalian hair, nail, and horn).[24–27] However, in GTCs, IF proteins assemble into 12-nm IFs during early stages of growth but later undergo a phase transition, where individual IFs condense with their neighbors into a much larger IF superstructure.[10,28] Such a process may be responsible for the near-isometry of thread dimensions (Figures 3A and 3B), where larger GTCs likely undergo a prolonged growth period, during which the length and diameter of threads increase at similar rates during phosphorylation.[11,29]

A brief comparison of slime threads to other intracellular polymers underscores how massive slime threads are (Figure 4C). The dimensions of slime threads far exceed those of other intracellular polymers such as intermediate filaments, microtubules, and filamentous actin (diameters ranging 7–24 nm; lengths up to a few tens of micrometers), and they are comparable to biofibers produced by extracellular or multicellular means, such as keratin fibers and arthropod silks, both of which involve the

coordination among numerous cells.[24,25] Mammals produce large keratin fibers via mechanisms that involve the sacrifice and joining together of large numbers of cells enriched in IFs and other structural proteins, while GTCs produce fibers that are nearly as large within a single cell.

The functions of thread production and storage are critical for GTCs to overcome various size constraints. One constraint that is believed to limit cell size is the detrimental effect that increasing cell volume has on intracellular transport and metabolism.[2] GTCs are unlike most cells in that a massive protein polymer takes up the vast majority of their cytoplasm. In mature GTCs, this polymer is most likely metabolically inert, and thus the volume of metabolically active cytoplasm may be effectively much smaller. A similar effect may explain the large size of adipocytes (fat cells), where most of the cytoplasm is occupied by oil droplets. On the other hand, there are good reasons to believe that GTCs have high metabolic rates given the amount of protein synthesis that must happen to produce the skein. A brief consideration of GTC growth rates illustrates this point. Based on the known refilling rate of slime glands in Pacific hagfish (*E. stoutii*), we estimate a minimum of ~33 times increase in skein volume (when L_S increases from 50 to 160 μm) over a period of 28 days,[30] with an average growth rate of ~780 μm^3/h. Also, it is worth noting that GTCs are potentially nourished by a network of thin cells called gland interstitial cells within the slime glands.[31] While the function of these cells has not been elucidated, one reasonable hypothesis is that they serve as nurse cells, and the metabolic support they provide allows GTCs to achieve larger sizes than they otherwise could.

Here, we have described a case of strong allometric scaling in a specialized defensive cell in hagfishes. Our results and analysis demonstrate that hagfish GTCs are some of the largest metabolically active cells in animals, as driven by selection for longer and thicker slime threads. Future studies may correlate the development and performance of slime threads and their variations in different sized species to further identify the principles underlying the evolutionary, developmental, and cellular mechanisms of the extreme size and allometry.

STAR★METHODS

Detailed methods are provided in the online version of this paper and include the following:

- KEY RESOURCES TABLE
- RESOURCE AVAILABILITY
  - Lead contact
  - Materials availability
  - Data and code availability
- EXPERIMENTAL MODEL AND SUBJECT DETAILS
- METHOD DETAILS
  - Specimen sampling
  - Image processing
- QUANTIFICATION AND STATISTICAL ANALYSIS
  - Scaling of GTC skeins with body size
  - Scaling of thread size with body size
  - Thread geometry models
  - Phylogenetically justified statistical analyses

SUPPLEMENTAL INFORMATION

Supplemental information can be found online at https://doi.org/10.1016/j.cub.2021.08.066.

ACKNOWLEDGMENTS

We thank Andrew Lowe for logistical help. Thanks also to Ben Frable, H.J. Walker, and Phil Hastings at the Scripps Institute of Oceanography (SIO) for access to specimens and Phil Zerofski at SIO for advice about trapping hagfishes in deep water. Michael Mincarone, Bo Fernholm, Charlene McCord, John Gregg, and Tim Winegard assisted with skein collection from Galapagos hagfishes. This study was supported by NSF grants IOS-1755397 to D.F. and IOS-1755337 to D.P.

AUTHOR CONTRIBUTIONS

Y.Z., S.P., K.N., and D.F. devised experiments. Y.Z., S.P., and K.N. performed the majority of data collection. Y.Z., S.P., K.N., and D.F. performed the majority of data analyses. D.P. contributed to phylogenetic analyses. All authors contributed to writing of the manuscript.

DECLARATION OF INTERESTS

The authors declare no competing interests.

Received: March 24, 2021
Revised: June 28, 2021
Accepted: August 26, 2021
Published: September 20, 2021

REFERENCES

1. Amodeo, A.A., and Skotheim, J.M. (2016). Cell-size control. Cold Spring Harb. Perspect. Biol. *8*, a019083.
2. Miettinen, T.P., and Björklund, M. (2017). Mitochondrial function and cell size: an allometric relationship. Trends Cell Biol. *27*, 393–402.
3. Downing, S.W., Spitzer, R.H., Salo, W.L., Downing, J.S., Saidel, L.J., and Koch, E.A. (1981). Threads in the hagfish slime gland thread cells: organization, biochemical features, and length. Science *212*, 326–328.
4. Downing, S.W., Salo, W.L., Spitzer, R.H., and Koch, E.A. (1981). The hagfish slime gland: a model system for studying the biology of mucus. Science *214*, 1143–1145.
5. Fudge, D.S., Levy, N., Chiu, S., and Gosline, J.M. (2005). Composition, morphology and mechanics of hagfish slime. J. Exp. Biol. *208*, 4613–4625.
6. Lim, J., Fudge, D.S., Levy, N., and Gosline, J.M. (2006). Hagfish slime ecomechanics: testing the gill-clogging hypothesis. J. Exp. Biol. *209*, 702–710.
7. Zintzen, V., Roberts, C.D., Anderson, M.J., Stewart, A.L., Struthers, C.D., and Harvey, E.S. (2011). Hagfish predatory behaviour and slime defence mechanism. Sci. Rep. *1*, 131.
8. Böni, L.J., Zurflüh, R., Baumgartner, M.E., Windhab, E.J., Fischer, P., Kuster, S., and Rühs, P.A. (2018). Effect of ionic strength and seawater cations on hagfish slime formation. Sci. Rep. *8*, 9867.
9. Naisbit, R.E., Kehrli, P., Rohr, R.P., and Bersier, L.F. (2011). Phylogenetic signal in predator-prey body-size relationships. Ecology *92*, 2183–2189.
10. Downing, S.W., Spitzer, R.H., Koch, E.A., and Salo, W.L. (1984). The hagfish slime gland thread cell. I. A unique cellular system for the study of intermediate filaments and intermediate filament-microtubule interactions. J. Cell Biol. *98*, 653–669.
11. Spitzer, R.H., Koch, E.A., and Downing, S.W. (1988). Maturation of hagfish gland thread cells: composition and characterization of intermediate filament polypeptides. Cell Motil. Cytoskeleton *11*, 31–45.
12. Koch, E.A., Spitzer, R.H., Pithawalla, R.B., Castillos, F.A., 3rd, and Parry, D.A. (1995). Hagfish biopolymer: a type I/type II homologue of epidermal keratin intermediate filaments. Int. J. Biol. Macromol. *17*, 283–292.

13. Fudge, D.S., Gardner, K.H., Forsyth, V.T., Riekel, C., and Gosline, J.M. (2003). The mechanical properties of hydrated intermediate filaments: insights from hagfish slime threads. Biophys. J. *85*, 2015–2027.
14. Fudge, D.S., and Gosline, J.M. (2004). Molecular design of the α-keratin composite: insights from a matrix-free model, hagfish slime threads. Proc. Biol. Sci. *271*, 291–299.
15. Mincarone, M.M., Plachetzki, D., McCord, C.L., Winegard, T.M., Fernholm, B., Gonzalez, C.J., and Fudge, D.S. (2021). Review of the hagfishes (Myxinidae) from the Galapagos Islands, with descriptions of four new species and their phylogenetic relationships. Zool. J. Linn. Soc. *192*, 453–474.
16. Gorbman, A. (1997). Hagfish development. Zool. Sci. *14*, 375–390.
17. Savage, V.M., Allen, A.P., Brown, J.H., Gillooly, J.F., Herman, A.B., Woodruff, W.H., and West, G.B. (2007). Scaling of number, size, and metabolic rate of cells with body size in mammals. Proc. Natl. Acad. Sci. USA *104*, 4718–4723.
18. Fernholm, B.O. (1998). Hagfish systematics. In The Biology of Hagfishes, , J.M. Jørgensen, J.P. Lomholt, R.E. Weber, and H. Malte, eds. (Springer), pp. 33–44.
19. Martini, F.H. (1998). The ecology of hagfishes. In The Biology of Hagfishes, , J.M. Jørgensen, J.P. Lomholt, R.E. Weber, and H. Malte, eds. (Springer), pp. 57–77.
20. Labonte, D., Clemente, C.J., Dittrich, A., Kuo, C.-Y., Crosby, A.J., Irschick, D.J., and Federle, W. (2016). Extreme positive allometry of animal adhesive pads and the size limits of adhesion-based climbing. Proc. Natl. Acad. Sci. USA *113*, 1297–1302.
21. Malda, J., de Grauw, J.C., Benders, K.E., Kik, M.J., van de Lest, C.H., Creemers, L.B., Dhert, W.J., and van Weeren, P.R. (2013). Of mice, men and elephants: the relation between articular cartilage thickness and body mass. PLoS ONE *8*, e57683.
22. Ortlepp, C., and Gosline, J.M. (2008). The scaling of safety factor in spider draglines. J. Exp. Biol. *211*, 2832–2840.
23. Kramer, A., and Francis, L. (2004). Predation resistance and nematocyst scaling for *Metridium senile* and *M. farcimen*. Biol. Bull. *207*, 130–140.
24. Fraser, R.D., MacRae, T.P., Parry, D.A., and Suzuki, E. (1986). Intermediate filaments in alpha-keratins. Proc. Natl. Acad. Sci. USA *83*, 1179–1183.
25. Marshall, R.C., Orwin, D.F.G., and Gillespie, J.M. (1991). Structure and biochemistry of mammalian hard keratin. Electron Microsc. Rev. *4*, 47–83.
26. Kreplak, L., and Fudge, D. (2007). Biomechanical properties of intermediate filaments: from tissues to single filaments and back. BioEssays *29*, 26–35.
27. Hu, J., Li, Y., Hao, Y., Zheng, T., Gupta, S.K., Parada, G.A., Wu, H., Lin, S., Wang, S., Zhao, X., et al. (2019). High stretchability, strength, and toughness of living cells enabled by hyperelastic vimentin intermediate filaments. Proc. Natl. Acad. Sci. USA *116*, 17175–17180.
28. Winegard, T., Herr, J., Mena, C., Lee, B., Dinov, I., Bird, D., Bernards, M., Jr., Hobel, S., Van Valkenburgh, B., Toga, A., and Fudge, D. (2014). Coiling and maturation of a high-performance fibre in hagfish slime gland thread cells. Nat. Commun. *5*, 3534.
29. Spitzer, R.H., Downing, S.W., Koch, E.A., Salo, W.L., and Saidel, L.J. (1984). Hagfish slime gland thread cells. II. Isolation and characterization of intermediate filament components associated with the thread. J. Cell Biol. *98*, 670–677.
30. Schorno, S., Gillis, T.E., and Fudge, D.S. (2018). Cellular mechanisms of slime gland refilling in Pacific hagfish (*Eptatretus stoutii*). J. Exp. Biol. *221*, jeb183806.
31. Fudge, D.S., Schorno, S., and Ferraro, S. (2015). Physiology, biomechanics, and biomimetics of hagfish slime. Annu. Rev. Biochem. *84*, 947–967.
32. R Core Team (2014). R: A language and environment for statistical computing (R Foundation for Statistical Computing).
33. Rueden, C.T., Schindelin, J., Hiner, M.C., DeZonia, B.E., Walter, A.E., Arena, E.T., and Eliceiri, K.W. (2017). ImageJ2: ImageJ for the next generation of scientific image data. BMC Bioinformatics *18*, 529.
34. McCord, C.L., Whiteley, E., Liang, J., Trejo, C., Caputo, R., Itehua, E., Hasan, H., Hernandez, S., Jagnandan, K., and Fudge, D. (2020). Concentration effects of three common fish anesthetics on Pacific hagfish (*Eptatretus stoutii*). Fish Physiol. Biochem. *46*, 931–943.
35. Froese, R., and Pauly, D. (2021). FishBase. https://www.fishbase.se/.
36. ObjectJ. (2021). https://sils.fnwi.uva.nl/bcb/objectj/.
37. Pagel, M. (1999). Inferring the historical patterns of biological evolution. Nature *401*, 877–884.
38. Revell, L.J. (2012). phytools: an R package for phylogenetic comparative biology (and other things). Methods Ecol. Evol. *3*, 217–223.
39. Paradis, E., Claude, J., and Strimmer, K. (2004). APE: analyses of phylogenetics and evolution in R language. Bioinformatics *20*, 289–290.
40. Hadfield, J.D. (2010). MCMC methods for multi-response generalized linear mixed models: the MCMCglmm R package. J. Stat. Softw. *33*, 1–22.
41. Hadfield, J.D., and Nakagawa, S. (2010). General quantitative genetic methods for comparative biology: phylogenies, taxonomies and multi-trait models for continuous and categorical characters. J. Evol. Biol. *23*, 494–508.

STAR★METHODS

KEY RESOURCES TABLE

REAGENT or RESOURCE	SOURCE	IDENTIFIER
Chemicals, peptides, and recombinant proteins		
Clove Oil	Sigma-Aldrich	C8392
MS-222 (powder; tricaine methanesulfonate)	Western Chemical, Ferndale, WA, USA	Cat# NC0135573
Sodium Citrate	Fisher Scientific	S279
Software and algorithms		
R 3.1	[32]	https://www.r-project.org/
ImageJ 2	[33]	https://imagej.nih.gov/ij/
ObjectJ	Norbert Nischer & Stelian Nastase, University of Amsterdam	https://sils.fnwi.uva.nl/bcb/objectj/
Other		
Square Pulse Stimulator	Grass Instruments	S48
Optical Microscope	Zeiss	Axio Imager 2

RESOURCE AVAILABILITY

Lead contact

Further information and requests for resources and reagents should be directed to and will be fulfilled by the lead contact, Yu Zeng (dreavoniz9@gmail.com).

Materials availability

This study did not generate new unique reagents.

Data and code availability

The datasets generated during this study are available at Data S1.

The code supporting the current study is available from the corresponding author on request.

Any additional information required to reanalyze the data reported in this work paper is available from the Lead Contact upon request.

EXPERIMENTAL MODEL AND SUBJECT DETAILS

We sampled from 87 individuals from 19 species of hagfishes (Data S1A). For sampling in the laboratory, wild-captured hagfishes were housed in a 1000-l tank filled with chilled artificial seawater (ASW; 34%, 8°C) at Chapman University, CA, USA. For sampling in the field, wild-captured hagfishes were anesthetized in 200 mg/L of clove oil following a previously established protocol[34] and subsequently euthanized with MS-222 (250mg/L) after experiments. Hagfishes are not covered under the Chapman University Institutional Animal Care and Use Committee (IACUC). All animal protocols used for this research were based on guidelines of the Canadian Council on Animal Care (https://www.ccac.ca/en/standards/guidelines/).

METHOD DETAILS

Specimen sampling

We sampled from 87 individuals from 19 species of hagfishes. Body length, mass, and slime exudate were sampled from captive hagfishes at Chapman University, from six species of wild-caught hagfishes from the Galapagos Islands, and from preserved specimens at the Scripps Institution of Oceanography Marine Vertebrates collection (Data S1A). Data for species-specific maximum body length was obtained from FishBase[35] and primary literature (Data S1B).

Because the body size of some specimens was measured fresh and others in the preserved state, we calculated a shrinkage factor (i.e., the ratio of body length in preserved specimen to that of the fresh specimen) from three preserved museum specimens (*E. carlhubbsi*, N = 2; *E. hexatrema*, N = 1) for which the fresh length was recorded at the time of capture. The mean shrinkage for

these specimens was 6.90 ± 0.03% (mean ± SD). This information was used to approximate the original body length of preserved specimens for which fresh body length was never recorded.

For fresh exudate samples, hagfishes were anesthetized in 200 mg/L of clove oil following McCord et al.[34] The animal was then transferred to a chilled dissection tray and measured for body length and mass. A Grass S48 Square Pulse Stimulator with a two-prong stimulation wand was used to induce the release of slime exudate from two to three glands posterior to the most posterior gill aperture.[31] Slime exudate was then collected in a 1.5 mL microcentrifuge tube with 0.5 M sodium citrate to prevent unravelling. For preserved samples, a small piece of skin containing a small number of slime glands (2 × 2 cm) was cut from the specimen and preserved in 70% ethanol. Gland thread cells were collected from these preserved slime glands by microdissection and stored in 1.5 mL microcentrifuge tubes at 4°C until their size was measured.

Image processing

To collect images of skeins for analysis, 10–20 μL of exudate was placed on a microscope slide and observed using a Zeiss Axio Imager 2 optical microscope. Images were taken under two magnifications for measuring skein dimensions and thread size. For skein dimensions, images were taken with transmitted light using a 5 × objective lens, with images typically containing 25–70 skeins (Figure S1D). Samples in which skeins were deformed from mechanical perturbation or exposure to low osmolarity solutions were omitted from our analysis. The major and minor axes of skeins (length L_S and width W_S, respectively) were measured from captured images using ObjectJ,[36] which allowed automatic analysis followed by manual proofreading in ImageJ,[33] The accuracy of this method was further validated by comparing with manually measured results (Figure S1C). For thread diameter (ϕ) measurements, images were taken with differential interference contrast (DIC) using a 40 × objective and focusing on the surface of skein, near the skein midpoint, where thread diameter is greatest (Figure S1E).[5] To provide a comparison against other hagfish cell types, we also sampled skin adipocytes and hepatocytes from 9 species of hagfishes and three types of epidermal cells (small mucus cell, large mucus cell and epidermal thread cell) from both juvenile and adult Pacific Hagfish (*E. stoutii*; body size ranges 11 – 40 cm; Data S1C).

QUANTIFICATION AND STATISTICAL ANALYSIS

All scaling analyses were conducted using generalized linear model ('glm') function in R.[32] Data were summarized as means ± SD unless otherwise specified.

Scaling of GTC skeins with body size

The size of skeins increases with the age of the GTC and thus varies within glands.[30] To minimize variability, we restricted our scaling analysis to mature skeins only, which we defined as the largest 5% and 20% of skeins from each sample. The power-law scaling of the GTC skein length (L_S) with body length (L) can be expressed as:

$$L_S = C_1 L^{b1} \quad \text{(Equation 8)}$$

where $\boldsymbol{C}_1$ is the slope coefficient and $\boldsymbol{b}1$ is the scaling exponent. The genus-specific and general power-law models were found by fitting a generalized linear model on log-transformed data in R (Table S3). The shape of an ellipsoidal skein can be characterized by an aspect ratio (*AR*):

$$AR = \frac{L_S}{W_S} \quad \text{(Equation 9)}$$

where L_S is skein length and W_S is skein width, corresponding with the major and minor axes of the ellipsoid-shaped skein, respectively.

In a mature GTC, the skein takes up the vast majority of the cell's volume,[3] and thus skein size is a good proxy of mature GTCs size. Skeins (and thus GTCs) were modeled as ellipsoids, with the volume approximated as:

$$V_S = \frac{1}{6}\pi L_S W_S^2$$

$$= \frac{1}{6}\pi L_S^3 AR^{-2}. \quad \text{(Equation 10)}$$

For comparison of GTCs with cells from other taxa, we collected volume and size data for cells from other vertebrate groups, mainly fish and mammals, from the literature (Data S1C).

Scaling of thread size with body size

The power-law scaling of thread diameter (ϕ) with skein length (L_S) was described using:

$$\phi = C_2 L_S^{b2} \quad \text{(Equation 11)}$$

where $\boldsymbol{C}_2$ is the slope coefficient and $\boldsymbol{b}2$ is the scaling exponent. Combining Equations 8 and 11, we derived the scaling of the thread diameter with body length:

$$\phi = C_2 C_1^{b2} L^{b1+b2} \quad \text{(Equation 12)}$$

In this study, we did not directly measure thread length (L_T) due to formidable technical obstacles.[5] However, thread length can be approximated by measuring maximum thread diameter, skein length and width, and making some reasonable assumptions about packing efficiency and the degree of thread taper.[3,5]

Here, we used the model developed by Downing et al.[3] to estimate thread length and modified it in light of the finding by Fudge et al.[5] that slime threads exhibit a substantial bidirectional taper (also see Figures S1F and S4A). From this model, L_T can be written as:

$$L_T = 0.996 \frac{P L_S W_S^2}{\phi_{max}^2} \quad \text{(Equation 13)}$$

where ϕ_{max} corresponds to the maximum thread diameter measured at the surface of the midpoint of skeins and $P = 90\%$ is the packing ratio, a conservative approximation of the volume percentage of thread within the GTC (see details of derivation in STAR Methods**)**. To address the covariation of thread length and diameter, we used an alternative model that assumed consistent skein geometry and thread geometry (i.e., consistent length to diameter ratio). Based on the volume of a skein $V = \frac{1}{6}\pi L_S W_S^2$ and a consistent aspect ratio, we have:

$$L_S W_S^2 \propto L_S^3 \propto \phi_{max}^2 L_T \quad \text{(Equation 14)}$$

Accordingly, we expected $L_S \propto \phi_{max} \propto L_T$ if the thread has consistent shape and undergoes isometric scaling with skein size. Based on this alternative model, we further expected $L_T \propto L_S^3$ with constant thread diameter and $\phi_{max} \propto L_S^{1.5}$ with constant thread length. Last, the relative length of thread to body size was defined as:

$$Q = \frac{L_T}{L} \quad \text{(Equation 15)}$$

Thread geometry models

Double-tapered model

In a previous study,[3] the total length of a thread was estimated by modeling a thread skein as an ellipsoid and the single thread as a uniformly tapered cylinder. A more recent study[5] indicated that the thread is double-tapered, with the diameters of the two thinner ends being 1/2 and 1/3 of the midpoint diameter (ϕ_{max}). Here, in light of both results, we modeled each thread as a combination of two longitudinally elongated conical frusta (Figure S1F). The conical frustum with $\phi_{min} = \frac{1}{2}\phi_{max}$ has the volume:

$$V_1 = \frac{7}{96}\pi L_T \phi_{max}^2 \approx 0.073 \pi L_T \phi_{max}^2 \quad \text{(Equation 16)}$$

and the other conical frustum with $\phi_{min} = \frac{1}{3}\phi_{max}$ has the volume:

$$V_2 = \frac{19}{216}\pi L_T \phi_{max}^2 \approx 0.088 \pi L_T \phi_{max}^2 \quad \text{(Equation 17)}$$

The total volume of a double-tapered thread is:

$$V = V_1 + V_2 = \frac{139}{864}\pi L_T \phi_{max}^2 \approx 0.161 \pi L_T \phi_{max}^2 \quad \text{(Equation 18)}$$

Next, with the assumption of an ellipsoidal shape, each thread skein has the volume of:

$$V = \frac{4}{3}\pi \left(\frac{L_S}{2}\right)\left(\frac{W_S}{2}\right)^2 = \frac{1}{6}\pi L_S W_S^2 \quad \text{(Equation 19)}$$

Equalizing Equations 18 and 19, we can express the thread length L_T as:

$$L_T \approx 0.966 \frac{P L_S W_S^2}{\phi_{max}^2} \quad \text{(Equation 20)}$$

where $P = 90\%$ is the packing ratio.

Single-tapered model

Downing et al.[3] estimated the total length of a thread by modeling the single thread as a single-tapered cylinder (Figure S1F), without incorporating the scaling relationship between thread diameter and skein size. For comparative purpose, similar to Equation 16, we have:

$$V = \frac{7}{48}\pi L_T \phi_{max}^2 \quad \text{(Equation 21)}$$

Combining Equations 21 and 19, we have:

$$L_T = \frac{8}{7}\frac{PL_S W_S^2}{\phi_{max}^2} \quad \text{(Equation 22)}$$

Thread length estimated using this model is ~19% longer than that estimated using the double-tapered model (Figure S6).

Phylogenetically justified statistical analyses

Correlational tests were conducted using R.[32] For phylogenetically justified analyses, we used the latest molecular phylogeny[15] (Figure S1B), which included 11 of 19 sampled species in this study. This phylogeny is non-ultrametric given the lack of hagfish fossils that can be used for calibrating the age of nodes. We calculated the phylogenetic signals (λ) for body and skein sizes using the maximum-likelihood approach implemented in Phytools.[37,38]

For the eight species that were not represented on the phylogeny, we added them as polytomous tips to the node representing the latest common ancestor at the genus level. We then generated 100 random trees with randomly resolved polytomous tips. Each new node was added using the function 'multi2 di' (package 'ape'),[39] and was given a branch length that was randomly drawn from a normal distribution of branch lengths with a mean of 0.1 × mean branch lengths of the original tree, and a standard deviation of 0.01 × the standard deviation of branch lengths from the original tree.

We analyzed two main correlations: skein length (L_S) versus body size (L), and maximum thread diameter (ϕ_{max}) versus skein length (L_S) within a phylogenetic context. To incorporate both inter- and intraspecific effects, we fit multivariate generalized linear mixed (GLMM) models using the ''MCMCglmm'' package (Monte Carlo Markov Chain generalized linear mixed model)[40] in R, with a Gaussian error distribution assumed for each variable. The phylogeny was fit as a random effect following previously developed methods[41] to calculate the inverse numerator relationship for phylogenetic effects. To address the influence of intraspecific variation, we compared the models with and without the specimen-specific identities as a random effect. For each analysis, we ran the MCMC chain for 1,000,000 iterations, with a burn-in of 250,000 and a thinning interval of 20, resulting in ~37500 effective samples of the posterior distribution of the parameters. The model fit was confirmed by ensuring that autocorrelation was low and the trait means lay within the 95% highest posterior density (HPD) intervals of the posterior predictive distribution of each trait. To assess the significance of the phylogenetic correlations, we calculated the posterior distribution of the correlation.

Current Biology, Volume *31*

Supplemental Information

Evolution of a remarkable intracellular polymer and extreme cell allometry in hagfishes

Yu Zeng, Skylar Petrichko, Kristen Nieders, David Plachetzki, and Douglas Fudge

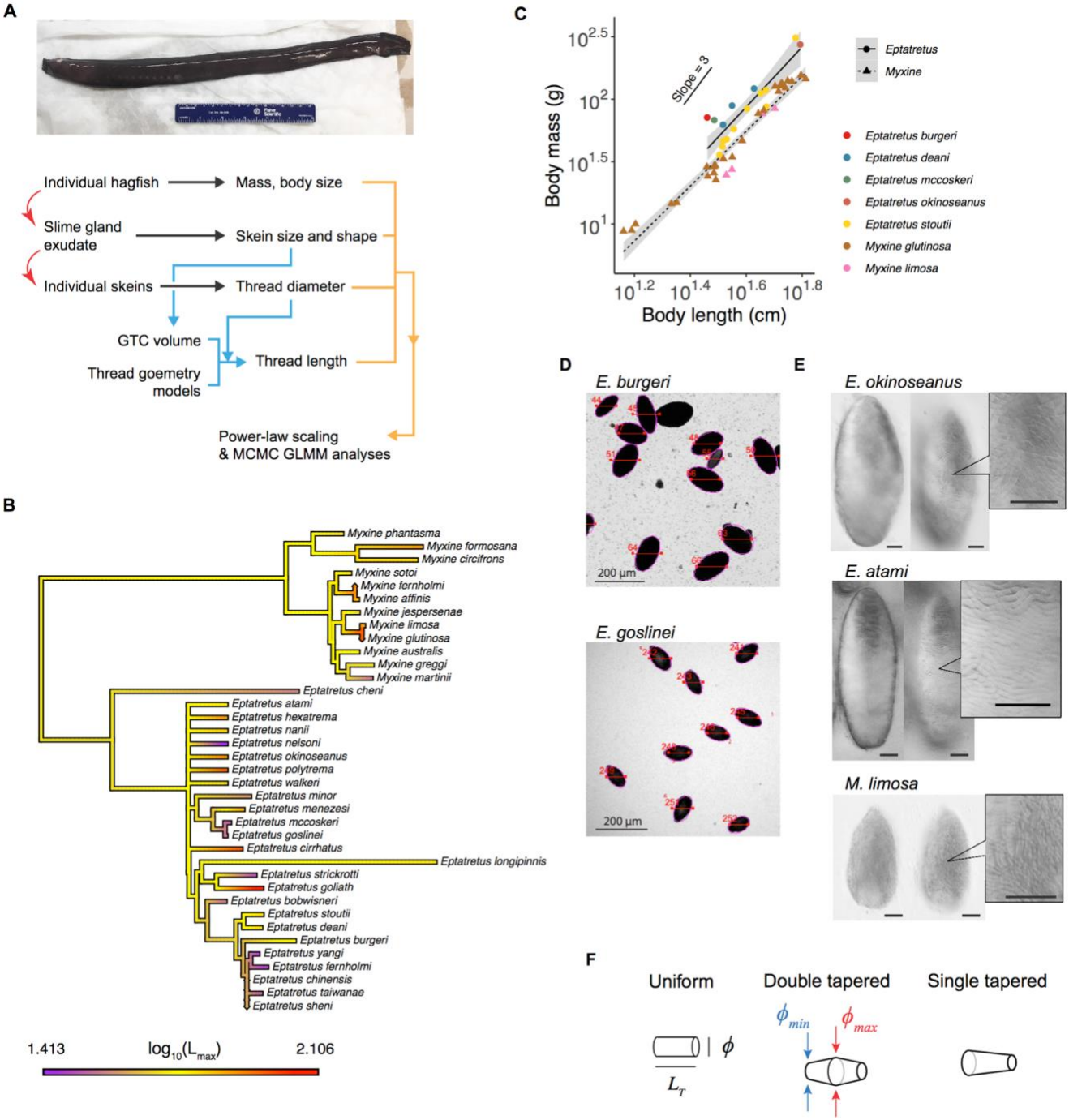
A
Individual hagfish
Mass, body size
Slime gland exudate
Skein size and shape
Individual skeins
Thread diameter
GTC volume
Thread goemetry models
Thread length
Power-law scaling & MCMC GLMM analyses
B
Myxine phantasma
Myxine formosana
Myxine circifrons
Myxine sotoi
Myxine fernholmi
Myxine affinis
Myxine jespersenae
Myxine limosa
Myxine glutinosa
Myxine australis
Myxine greggi
Myxine martinii
Eptatretus cheni
Eptatretus atami
Eptatretus hexatrema
Eptatretus nanii
Eptatretus nelsoni
Eptatretus okinoseanus
Eptatretus polytrema
Eptatretus walkeri
Eptatretus minor
Eptatretus menezesi
Eptatretus mccoskeri
Eptatretus goslinei
Eptatretus cirrhatus
Eptatretus longipinnis
Eptatretus strickrotti
Eptatretus goliath
Eptatretus bobwisneri
Eptatretus stoutii
Eptatretus deani
Eptatretus burgeri
Eptatretus yangi
Eptatretus fernholmi
Eptatretus chinensis
Eptatretus taiwanae
Eptatretus sheni
1.413
log10(Lmax)
2.106
C
Body mass (g)
Body length (cm)
Slope = 3
Eptatretus
Myxine
Eptatretus burgeri
Eptatretus deani
Eptatretus mccoskeri
Eptatretus okinoseanus
Eptatretus stoutii
Myxine glutinosa
Myxine limosa
D
E. burgeri
200 µm
E. goslinei
200 µm
E
E. okinoseanus
E. atami
M. limosa
F
Uniform
Double tapered
Single tapered

Figure S1. Morphometrics and phylogenetics of maximum body size, Related to Figure 1-2. (A) Workflow for data collection and analyses. The top image shows a Black Hagfish (*Eptatretus deani*). **(B)** Ancestral state reconstruction for maximum body length (L_{max}; unit, cm) on the latest hagfish phylogeny[S1] using the function 'contMap' (package 'phytools'[S2]). Note the repeated increases and decreases of L_{max}, corresponding with the wide range of variations shown in main text **Figure 1C**. The original phylogeny was pruned to show all the species examined in this study. Owing to the lack of hagfish fossils, we did not time-calibrate this phylogeny. Seven species not represented on the original tree were added as polytomous tips. See **Data S1B** for L_{max}. **(C)** Mass allometry in hagfishes sampled in this study. Across all animals, body mass (m) scales with body length (L) with an exponent 2.26±0.13 (mean±S.D.), corresponding with $L \propto m^{0.44}$. Data based on 51 individuals from 7 species (see **Data S1A**). For *Eptatretus*, scaling exponent = 2.40±0.31, slope coefficient = -1.91±0.50; for *Myxine*, scaling exponent = 2.20±0.09, slope coefficient = -1.77±0.14). Genus-specific regression models were used to predict body mass for individuals with no mass data. **(D)** Two sample images of skeins observed with transmitted light under 5× objective lens, with auto-fitted ellipses from the ObjectJ program for length and width measurements. We found no significant differences between automatically measured and manually measured data. **(E)** Exemplar skein images taken with differential interference contrast (DIC) under 40× objective lens, with two different focuses showing the skein profile and the threads on the outer surface. Enlarged areas show details of skein surface, which was used for thread diameter measurements. **(F)** Three different geometry models for slime threads, as shown in longitudinally compressed perspective.

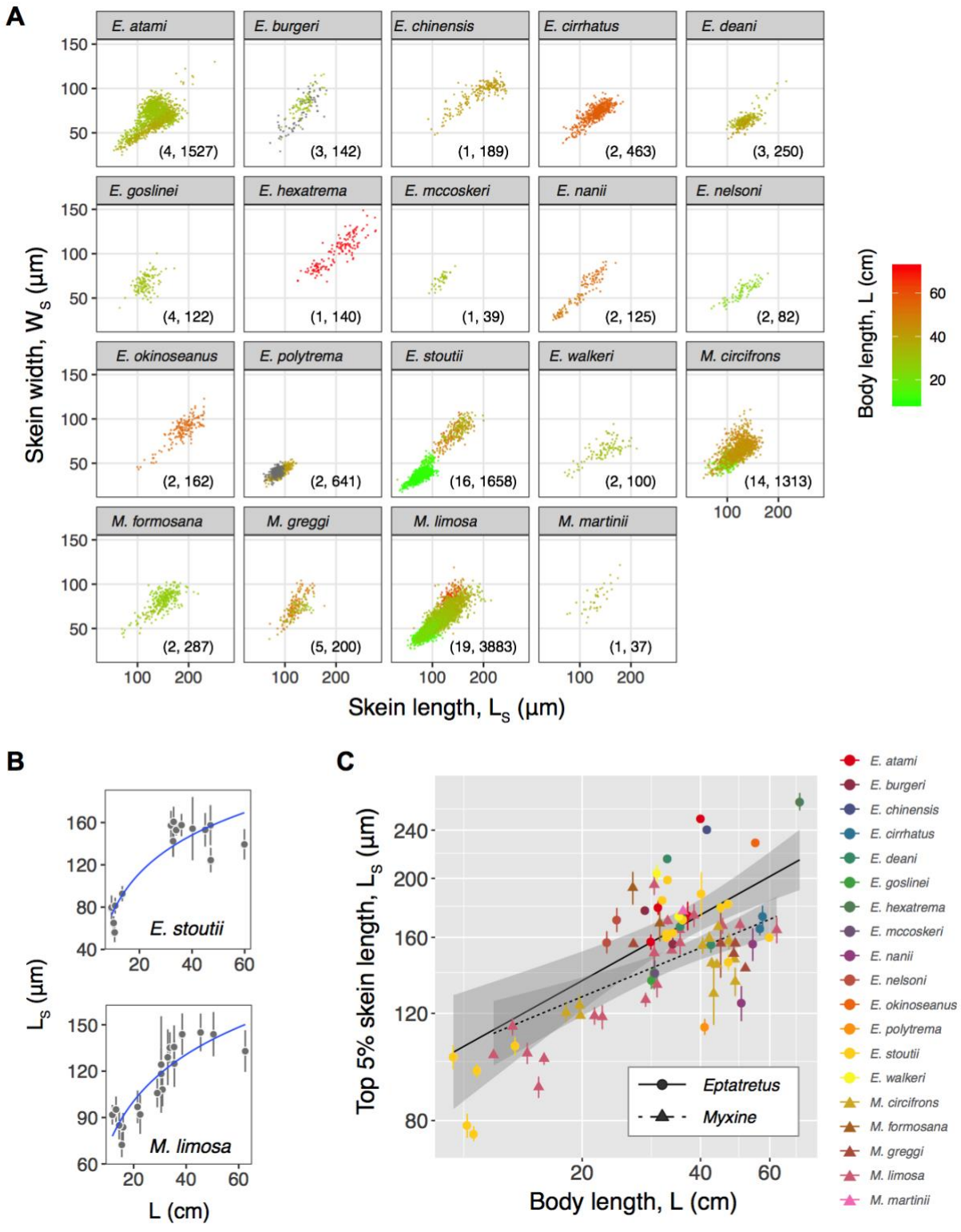
A
E. atami
E. burgeri
E. chinensis
E. cirrhatus
E. deani
E. goslinei
E. hexatrema
E. mccoskeri
E. nanii
E. nelsoni
E. okinoseanus
E. polytrema
E. stoutii
E. walkeri
M. circifrons
M. formosana
M. greggi
M. limosa
M. martinii
(4, 1527)
(3, 142)
(1, 189)
(2, 463)
(3, 250)
(4, 122)
(1, 140)
(1, 39)
(2, 125)
(2, 82)
(2, 162)
(2, 641)
(16, 1658)
(2, 100)
(14, 1313)
(2, 287)
(5, 200)
(19, 3883)
(1, 37)
Skein width, W_s (µm)
Skein length, L_s (µm)
Body length, L (cm)
B
E. stoutii
M. limosa
L_s (µm)
L (cm)
C
Top 5% skein length, L_s (µm)
Body length, L (cm)
Eptatretus
Myxine
E. atami
E. burgeri
E. chinensis
E. cirrhatus
E. deani
E. goslinei
E. hexatrema
E. mccoskeri
E. nanii
E. nelsoni
E. okinoseanus
E. polytrema
E. stoutii
E. walkeri
M. circifrons
M. formosana
M. greggi
M. limosa
M. martinii

Figure S2. Variation of GTC size, as represented by skein length, Related to Figure 2. (A) An overview of skein length (L_S) and skein width (W_S) for all sampled species. Points represent individual skeins, with color gradient representing body size (L; missing data shown in gray). Sample sizes (the number of animals and skeins, respectively) in parentheses. **(B)** The ontogenetic variation of L_S with respect to L in two species, with trend lines representing logarithmic regression models. **(C)** Skein length (L_S) from the largest 5% of GTCs sampled from each hagfish plotted against body size (L), exhibiting a negative allometry (scaling exponent: 0.37±0.04 for both genera combined, 0.41±0.06 for *Eptatretus* and 0.31±0.05 for *Myxine*; mean±s.e.m.) similar to the results in **Figure 2A**. Values are means±S.D.

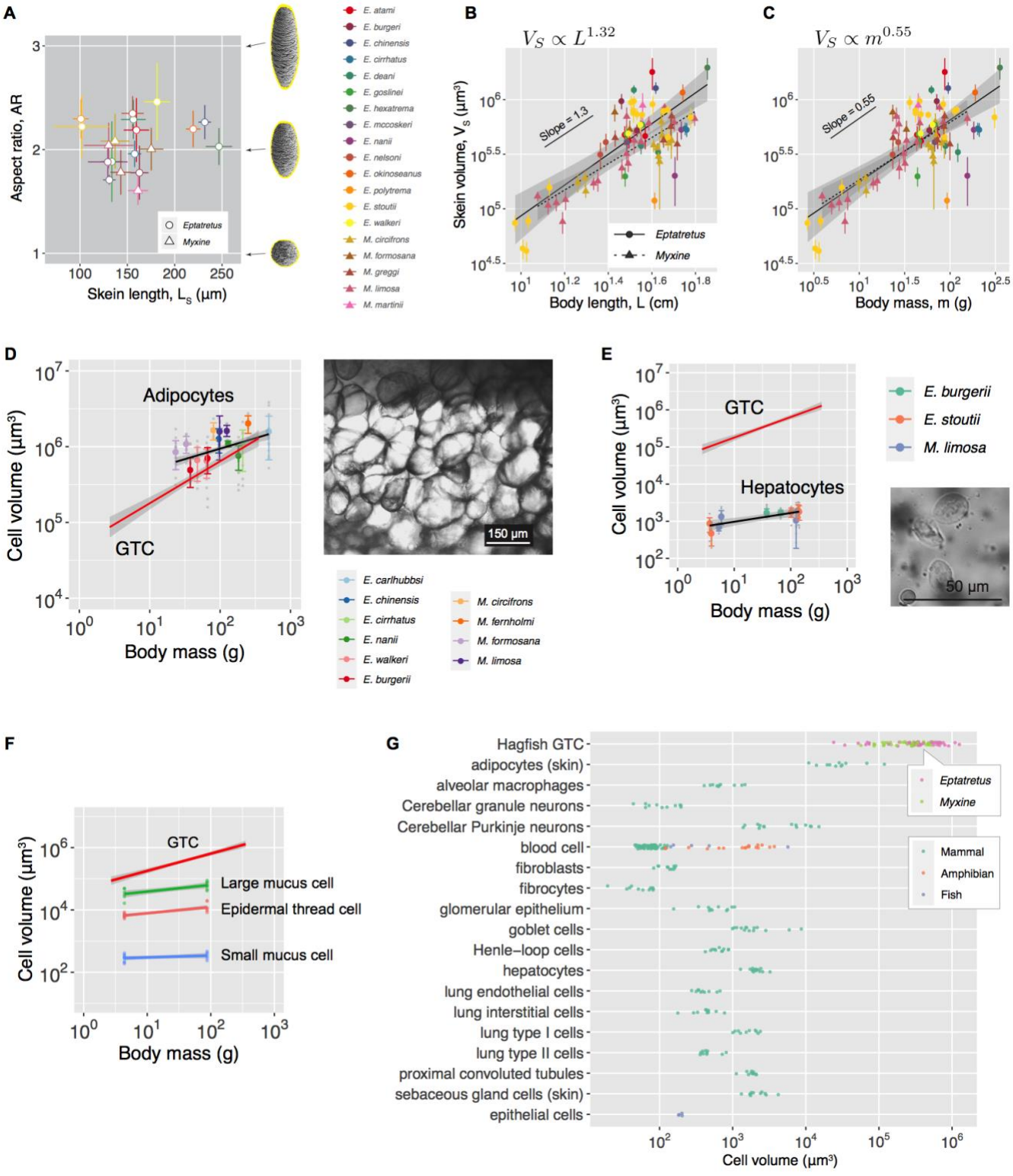
A
Aspect ratio, AR
Skein length, L_S (μm)
Eptatretus
Myxine
E. atami
E. burgeri
E. chinensis
E. cirrhatus
E. deani
E. goslinei
E. hexatrema
E. mccoskeri
E. nanii
E. nelsoni
E. okinoseanus
E. polytrema
E. stoutii
E. walkeri
M. circifrons
M. formosana
M. gregi
M. limosa
M. martinii
B
$V_S \propto L^{1.32}$
Slope = 1.3
Skein volume, V_S (μm³)
Body length, L (cm)
C
$V_S \propto m^{0.55}$
Slope = 0.55
Body mass, m (g)
D
Adipocytes
GTC
Cell volume (μm³)
Body mass (g)
150 μm
E. carlhubbsi
E. chinensis
E. cirrhatus
E. nanii
E. walkeri
E. burgerii
M. circifrons
M. fernholmi
M. formosana
M. limosa
E
GTC
Hepatocytes
Cell volume (μm³)
Body mass (g)
E. burgerii
E. stoutii
M. limosa
50 μm
F
GTC
Large mucus cell
Epidermal thread cell
Small mucus cell
Cell volume (μm³)
Body mass (g)
G
Hagfish GTC
adipocytes (skin)
alveolar macrophages
Cerebellar granule neurons
Cerebellar Purkinje neurons
blood cell
fibroblasts
fibrocytes
glomerular epithelium
goblet cells
Henle–loop cells
hepatocytes
lung endothelial cells
lung interstitial cells
lung type I cells
lung type II cells
proximal convoluted tubules
sebaceous gland cells (skin)
epithelial cells
Cell volume (μm³)
Eptatretus
Myxine
Mammal
Amphibian
Fish

Figure S3. Variations of GTC shape and size in relation to other cells, Related to Figure 2. (A) Plot shows species-specific average aspect ratio (AR) versus skein length. AR varied significantly between species (ANOVA, $F_{18,2267} = 33.64$, $P < 0.0001$), with the species-specific means ranging between 1.6 – 2.5. Values are means±S.D. Colors represent different species. See **Table S2** for phylogenetically justified analyses of variance. **(B)** shows the scaling of GTC volume with body size (L) (scaling exponent: 1.33±0.13 for both genera combined, 1.40±0.20 for *Eptatretus* and 1.20±0.15 for *Myxine*; mean±s.e.m.). **(C)** shows the scaling of GTC volume with body mass (m) (scaling exponent: 0.55±0.05 for both genera combined, 0.57±0.08 for *Eptatretus* and 0.53±0.07 for *Myxine*; mean±s.e.m.). For individuals lacking mass data, mass was predicted from body length using genus-specific linear models (**Figure S1C**). Data are from the top 20% largest skeins of each animal. See **Table S3** for more details. **(D)** Comparison of allometry between GTCs and adipocytes in hagfishes. Adipocytes were relatively large with a scaling exponent 0.24±0.04 ($P < 0.0001$; $N = 9$ species; see **Data S1D**), which is greater than the range of 0.13–0.17 exhibited by skin adipocytes and abdominal skin adipocytes in mammals (**Figure 2B**). Values are means ± S.D., with gray dots representing measured values. Inset shows the large skin adipocytes of an adult *M. limosa*. **(E)** Comparison of allometry between GTC and hepatocyte in hagfishes. Hepatocytes were sampled from ten individuals of three species (see **Data S1D**), showing an exponent of 0.26±0.03 ($P < 0.0001$). Values are means ± S.D., with gray dots representing measured values. Inset shows the hepatocytes from an adult *E. burgerii*. **(F)** Comparison of GTC size with three epidermal cells sampled from juvenile and adult Pacific hagfishes (*E. stoutii*). Large mucus cell (LMC) and epidermal thread cell (ETC) exhibited significant allometry (exponent 0.20 – 0.21), but small mucus cells (SMC) did not scale with body size. Scaling exponents: LMC, 0.21 ± 0.06, $P < 0.01$; SMC, 0.06 ± 0.04, $P > 0.1$; ETC, 0.20 ± 0.04, $P < 0.0001$. This preliminary sampling suggests a potentially different allometry pattern of hagfish cells from mammalian cells. The GTCs exhibited the largest scaling exponent among sampled cells. **(G)** A comparison of cell volume between hagfish GTCs and other vertebrate cells, where the volume of GTC is 1–4 orders of magnitude greater than that of the other cells. For hagfish GTCs, each dot represents the mean cell volume of the 20% largest GTCs; for other cells, dots represent species-specific mean cell volume (see **Data S1E**).

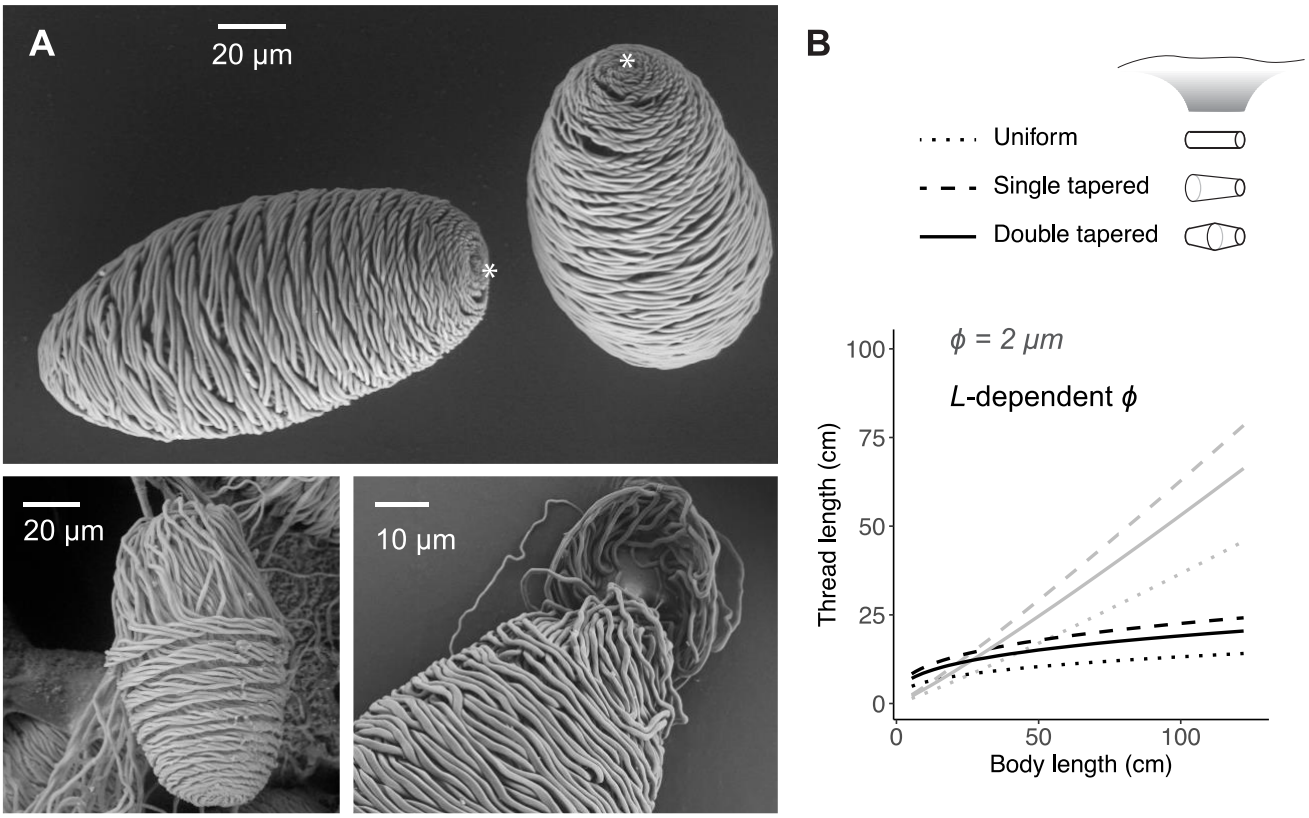

Figure S4. Variation of thread diameter and thread length estimation, Related to Figure 3. (A) Variation of thread diameter, as shown with scanning electron microscope (SEM) images of thread skeins of Pacific Hagfish (*E. stoutii*). Note the relatively uniform thread diameter and the tapering toward both ends of the cell, as noted by the asterisk symbols (see Fudge et al.[S3] and Winegard et al.[S4] for more details). Images courtesy of Gaurav Jain. **(B)** Comparison of thread length estimated using different geometry models. Gray lines represent the alternative model assuming a constant thread diameter ($\phi = 2$ µm). Line types represent different thread geometry models (shown with longitudinally condensed cartoons of threads). Thread length predicted using single-tapered model is ~19% longer than that predicted using double-tapered model. $AR = 2$ was assumed here. The model shows that if the largest skeins had small and constant thread diameter, they would have absurdly long threads.

						MLλ vs. λ=0		MLλ vs. λ=1	
Variable	***N***	**ML*λ***	***Lh* (MLλ)**	***Lh* (λ=0)**	***Lh* (λ=1)**	***LR***	***P***	***LR***	***P***
$L_{S,max}$	19	6.6e-05	-97.51	-97.51	-101.54	0	1	-8.1	< 0.005
L_{max}	19	6.6e-05	-75.37	-75.37	-78.61	0	1	-6.5	< 0.05

Table S1. Summary of the best model fits for the evolution of skein length ($L_{S,max}$; based on the top 20% largest GTC skeins) and maximum body length (L_{max}), Related to Figure 1-2. The maximum-likelihood model was compared with alternative models where the phylogenetic signal λ was forced to be 1 or 0. The best-fitting model was found using the likelihood ratio (LR) test: $LR = -2 \times (Lh_{better\ \ fitting\ model} - Lh_{worse\ \ fitting\ model})$, whereby the better fitting model has the highest log-likelihood score, Lh. Here, the small λ values reflect the large differences in body and skein sizes among closely related species, often associated with high rates of trait evolution.

Correlation	**Coefficient**	**λ posterior mean (95% HPD)**
L_S ~ L	0.71 (0.49, 0.95), ***	0.17 (1.2e-10, 0.56)
L_S ~ L †	0.71 (0.48, 0.94), ***	0.17 (3.3e-11, 0.56)
ϕ_{max} ~ L_S	0.76 (0.63, 0.89), ***	0.18 (1.9e-8, 0.53)
ϕ_{max} ~ L_S †	0.76 (0.63, 0.90), ***	0.18 (5.8e-8, 0.51)
ϕ_{max} ~ L_S †‡	0.76 (0.64, 0.90), ***	0.18 (1.6e-8, 0.1)

Table S2. Results of Monte Carlo Markov Chain generalized linear mixed model (MCMC GLMM) for two pairwise correlations, Related to Figure 2-3. Variables were $\log_{10}$-transformed and then scaled before analyses. Values are model-fit estimates, with 95% confidence intervals in brackets and asterisk symbols denoting the ranges of *P*-value (*, $P < 0.05$; ***, $P < 0.0001$). For phylogenetic signal λ of the residual errors, values are posterior means with the 95% highest posterior density (HPD) intervals in brackets. †, models in which individual hagfishes were treated as a random effect. ‡, models in which individual skeins were treated as a random effect.

	$\log_{10}(m) = a + b \cdot \log_{10}(L)$	
	a	b
Myxine	-1.77 (0.14), ***	2.20 (0.09), ***
Eptatretus	-1.91 (0.50), **	2.40 (0.32), ***
Overall	2.71 (0.06), ***	2.26 (0.13), ***

(mass ~ body length; units: m - g; L - m; a = $\log_{10}(C)$ as in Eqns. 8, 11, and 12 in Methods)

	$\log_{10}(L_S) = a + b \cdot \log_{10}(L)$	
	a	b
Myxine	2.28 (0.03), ***	0.30 (0.05), ***
Eptatretus	2.38 (0.03), ***	0.42 (0.06), ***
Overall	2.34 (0.02), ***	0.37 (0.04), ***

(skein length ~ body length; units: L_S - μm; L - m)

	$\log_{10}(AR) = a + b \cdot \log_{10}(L_S)$	
	a	b
Myxine	2.31 (0.21), ***	-0.002 (0.001)
Eptatretus	2.10 (0.17), ***	-0.0007 (0.0.0011)
Overall	2.10 (0.12), ***	-0.0008 (0.0008)

(skein aspect ratio ~ skein length; units: L_S - μm; based on individual-specific mean of top 20% largest skeins)

	$\log_{10}(\phi_{max}) = a + b \cdot \log_{10}(L_S)$	
	a	b
Myxine	-1.75 (0.12), ***	0.97 (0.06), ***
Eptatretus	-2.00 (0.09), ***	1.09 (0.04), ***
Overall	-1.90 (0.07), ***	1.04 (0.03), ***

(thread diameter ~ skein length; units: ϕ_{max} - μm; L_S - μm)

	$\log_{10}(V) = a + b \cdot \log_{10}(L)$	
	a	b
Myxine	3.73 (0.22), ***	1.20 (0.15), ***
Eptatretus	3.53 (0.30), ***	1.40 (0.20), ***
Overall	3.60 (0.30), ***	1.33 (0.13), ***

(skein volume ~ body size; units: V - μm^3; L - cm)

	$\log_{10}(V) = a + b \cdot \log_{10}(m)$	
	a	b
Myxine	4.73 (0.11), ***	0.53 (0.07), ***
Eptatretus	4.68 (0.15), **	0.57 (0.08), ***
Overall	4.70 (0.09), ***	0.55 (0.05), ***

(skein volume ~ body mass; units: V - μm^3; m - g; based on individual-specific mean of top 20% largest skeins)

Table S3. Power-law scaling models, Related to Figure 2-3. Each model-fit estimate is followed by standard errors in brackets; asterisk symbol denotes the ranges of *P*-value (**, $P < 0.01$; ***, $P < 0.0001$).

Supplemental References

S1. Mincarone, M. M., Plachetzki, D., McCord, C. L., Winegard, T. M., Fernholm, B., Gonzalez, C. J. and Fudge, D. S. (2021). Review of the hagfishes (Myxinidae) from the Galapagos Islands, with descriptions of four new species and their phylogenetic relationships. Zool. J. Linnean Soc. *192*, 453-474.

S2. Revell, L. J. (2012). phytools: an R package for phylogenetic comparative biology (and other things). Methods Ecol. Evol. *3*, 217-223.

S3. Fudge, D. S., Levy, N., Chiu, S. and Gosline, J. M. (2005). Composition, morphology and mechanics of hagfish slime. J. Exp. Biol. *208*, 4613-4625.

S4. Winegard, T., Herr, J., Mena, C., Lee, B., Dinov, I., Bird, D., Bernards, M., Hobel, S., Van Valkenburgh, B. and Toga, A. (2014). Coiling and maturation of a high-performance fibre in hagfish slime gland thread cells. Nat. Commun. *5*, 1-5.